CHEMISTRY
A European Journal

A Journal of
ChemPubSoc Europe

Accepted Article

Title: Majority-Rules Effect and Allostery in Molecular Recognition of Calix[4]arene-Based Triple-Stranded Metallohelicates

Authors: Yutaro Yamasaki, Hidemi Shio, Tomoko Amimoto, Ryo Sekiya, and Takeharu Haino

To be cited as: *Chem. Eur. J.* 10.1002/chem.201800997

Link to VoR: http://dx.doi.org/10.1002/chem.201800997

Supported by
ACES

WILEY-VCH

10.1002/chem.201800997

WILEY-VCH

FULL PAPER

Majority-Rules Effect and Allostery in Molecular Recognition of Calix[4]arene-Based Triple-Stranded Metallohelicates

Yutaro Yamasaki,[a] Hidemi Shio,[a] Tomoko Amimoto,[b] Ryo Sekiya,[a] and Takeharu Haino*[a]

Dedication ((optional))

Abstract: The triple-stranded metallohelicates **1a,b**–**3a,b** possessing the internal guest binding cavities surrounded by the calix[4]arene units were synthesized via the coordination-driven self-assembly. The UV/vis titration experiments verified that the metallohelicates encapsulated the *N*-methyl pyridinium cations bearing the amino acid groups to form the host-guest complexes. The guest chirality was transferred to the helicity of the helicates through the steric contact between the stereogenic center of the amino acid group and the metal cores. The (*M*)-helicity was induced when guests (*R*)-**4**–(*R*)-**6** were accommodated within the cavities. The multiple guest complexation within the self-assembled helicates **2a** and **3a** displayed large positive cooperative effects, indicating that the first guest complexation preorganizes the rest of the cavities to facilitate the subsequent guest binding. This cooperativity results in the majority-rules effect in the chiral guest binding for **2a** and **3a**.

Introduction

Helical structures are ubiquitous in nature.[1] Tobacco mosaic virus,[2] F-actin,[3] DNA,[4] and the α-helix peptide sequence[5] are typical examples of helical organization in a range of sizes extending from the nanometer to micron scales. These helical structures are key structural motifs that play a crucial role in the regulation of physiological functions.[6] Much effort has been devoted to mimicking the helical structures of biopolymers with artificial supramolecules and macromolecules in order to obtain unique photochemical and catalytic properties.[7] Compared to the single chain helical structures,[8] multi-stranded helical structures have been studied to a lesser extent due to the difficulties in their synthesis. Therefore, additional non-covalent interactions such as hydrogen bonding interaction, π-π stacking interaction, and dipole-dipole interaction are required to direct multi-stranded helical organizations.[9]

A coordination-driven self-assembly has become an alternative approach for the construction of multi-stranded helical structures, the so-called “metallohelicate.” In seminal work, Lehn and co-workers reported on a structurally characterized double-stranded metallohelicate using a bipyridine-copper(I) coordination bond.[10] Since then, metallohelicates have been actively investigated.[11],[12] The groups of Raymond,[13] Stack,[14] Albrecht,[15] and Hahn[16] synthesized triple-stranded metallohelicates formed through the self-assembly of catechol ligands with metal ions. The labile coordination bonds permit the dynamic interconversion between left-handed (*M*)- and right-handed (*P*)-forms, which can be biased by chiral guest complexation to the exterior of the helicates.[17] Despite the many examples of self-assembled multinuclear metallohelicates possessing conformationally coupled metal cores,[18] a limited number of majority-rules and allosteric effects have been demonstrated in the molecular recognition of multinuclear metallohelicates due to the lack of binding cavities large enough to encapsulate the sizable chiral guests.[19] Extended helicates possessing multiple guest-binding cavities are of particular interest (Figure 1a). Encapsulation of chiral guests in one of the cavities can bias the handedness of the helicates, and simultaneously regulate the rest of the cavities to drive the positive cooperativity for the inclusion of another guest.

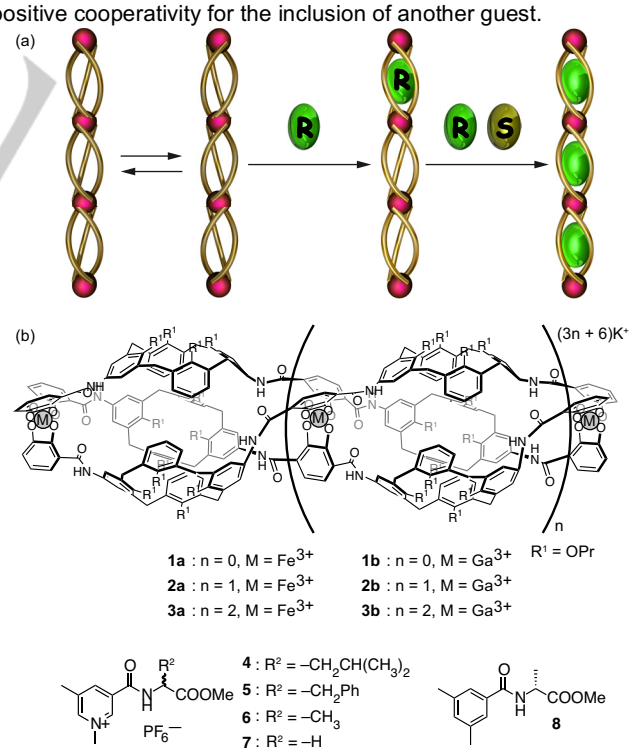

Figure 1. (a) Schematic representation of preorganization of conformationally coupled guest-binding cavities through guest encapsulation. (b) Structures of triple-stranded metallohelicates **1a,b**, **2a,b**, and **3a,b** and guests **4**–**8**.

[a] Y. Yamasaki, H. Shio, Prof. Dr. R. Sekiya, Prof. Dr. T. Haino
Department of Chemistry,
Graduate School of Science, Hiroshima University,
1-3-1 Kagamiyama, Higashi-Hiroshima, 739-8526 Japan
E-mail: haino@hiroshima-u.ac.jp
[b] T. Amimoto
Natural Science Center for Basic Research and Development,
Hiroshima University,
1-3-1 Kagamiyama, Higashi-Hiroshima 739-8526, Japan

Supporting information for this article is given via a link at the end of the document.((Please delete this text if not appropriate))

10.1002/chem.201800997

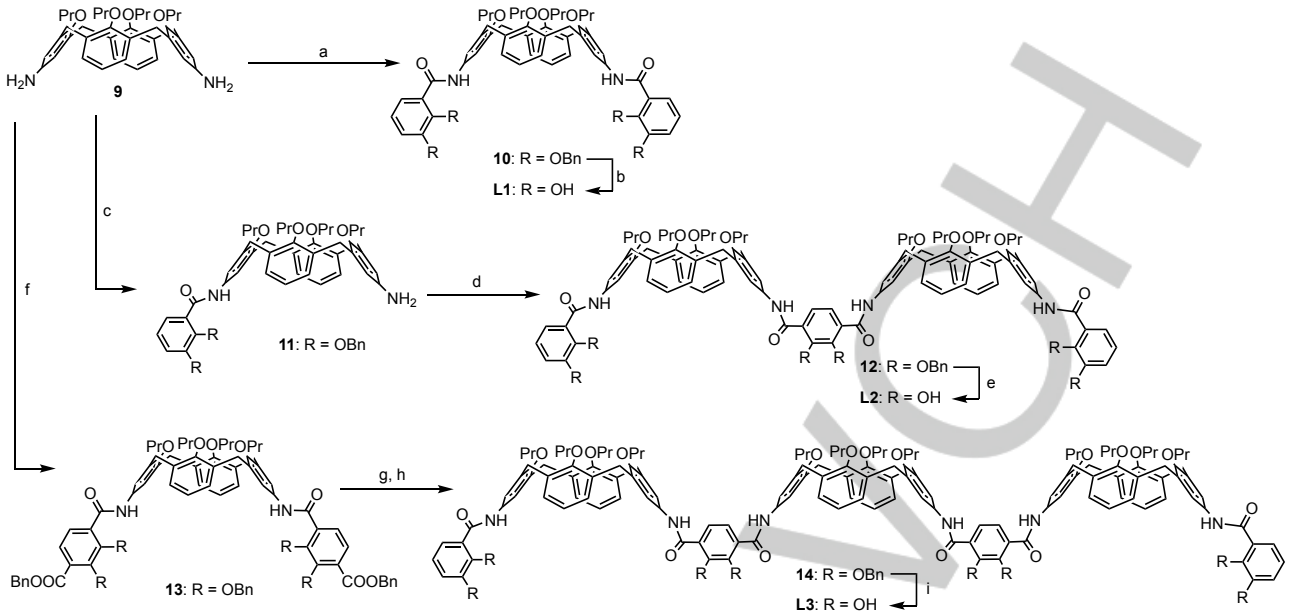

Scheme 1. Synthesis of **L1**, **L2**, and **L3**. Reagents and conditions: (a) 2,3-bis(benzyloxy)benzoic acid, EDC, HOBt, DMF, 85%; (b) H_2, Pd/C, 25% AcOEt–THF, 89%; (c) 2,3-bis(benzyloxy)benzoic acid, EDC, HOBt, DMF, 21%; (d) 2,3-bis(benzyloxy)telephthalic acid, EDC, HOBt, DMF, 77%; (e) H_2, Pd/C, 25% AcOEt–THF, 88%; (f) 2,3-bis(benzyloxy)telephthalic acid monobenzyl ester, EDC, HOBt, DMF, 63%; (g) LiOH, 30% H_2O–THF, 69%; (h) **11**, EDC, HOBt, DMF, 87%; (i) H_2, Pd/C, THF, 67%.

We have previously reported a D_3-symmetric dinuclear triple-stranded helicates **1a,b** composed of trivalent metal ions and di-anionic form of C_2-symmetric calix[4]arene-based bis-bidentate ligands **L1** (Scheme 1).[20] Herein, we report the synthesis and the molecular recognition of multinuclear triple-stranded supramolecular helicates **1a,b**, **2a,b**, and **3a,b** possessing one, two and three guest-binding cavities (Figure 1b). The *N*-methylpyridinium guests **4**–**7** bearing chiral amino acids were captured into the cavities. The conformationally coupled multiple cavities of **2a** and **3a** displayed strong cooperativity in the guest binding. The guest chirality was effectively transferred to the helical senses of the helicates through the steric interaction between the cavities and the stereogenic centers of the guests. Majority-rules effects were found in the guest binding for helicates **2a** and **3a**.

Results and Discussion

Synthesis of calix[4]arene ligands

The syntheses of ligands **L1**–**L3** are outlined in Scheme 1. Ligand **L1** was prepared from 5,17-diaminocalix[4]arene **9**[21] in accordance with our previously reported method.[20] The condensation reaction of **9** and 2,3-bis(benzyloxy)benzoic acid gave the protected calix[4]arene **10**, which was deprotected to afford the monomeric ligand **L1** in excellent yield. Ligand **L2** was synthesized from **9**. The mono-substituted calix[4]arene **11** was produced through the condensation of **9** with one equivalent of 2,3-bis(benzyloxy)benzoic acid. The treatment of **11** with 0.5 equivalents of 2,3-bis(benzyloxy)telephthalic acid gave biscalix[4]arene **12**, which was subjected to hydrogenolysis in the presence of Pd/C under hydrogen atmosphere to furnish **L2** in good yield. **L3** was also prepared from compound **9**. The condensation reaction of **9** with two equivalents of 2,3-bis(benzyloxy)telephthalic acid monobenzyl ester afforded the disubstituted calix[4]arene **13** in 63% yield. The hydrolysis of **13** with LiOH, and the following condensation reaction with two equivalents of **11** resulted in triscalix[4]arene **14** in 60% yield. The hydrogenolysis of **14** in the presence of Pd/C under hydrogen atmosphere afforded **L3** in good yield.

Coordination-Driven Self-Assembly

The deprotonation of **L1**, **L2**, and **L3** with KOH in methanol gave the anionic ligands $\mathbf{L1}^{2-}$, $\mathbf{L2}^{3-}$, and $\mathbf{L3}^{4-}$, which were treated with $Fe(acac)_3$ or $Ga(acac)_3$. The absorptions of K_2**L1**, K_3**L2**, and K_4**L3** appeared approximately at 290 nm (Figures 2a,b,c). The addition of $Fe(acac)_3$ decreased the intensity of the absorption bands, and new absorption bands emerged in the ranges of 270–280 nm and 520–600 nm with isosbestic points for $\mathbf{L1}^{2-}$, $\mathbf{L2}^{3-}$, and $\mathbf{L3}^{4-}$. The visible absorption bands correspond to the ligand-to-metal charge transfer (LMCT) in the [tris(catecholato)iron(III)]$^{3-}$ complexes, which are responsible for the formation of the self-assembled metallohelicates.[22] The metal-ligand stoichiometric ratios for **1a**, **2a**, and **3a** were determined using a Job plot (Figure 2d). The plot showed the peaks appearing at the mole ratios of 3:2, 1:1, and 3:4 for K_2**L1**, K_3**L2**, and K_4**L3**, respectively, confirming the formation of the triple-stranded helicates **1a**, **2a**, and **3a**.

10.1002/chem.201800997

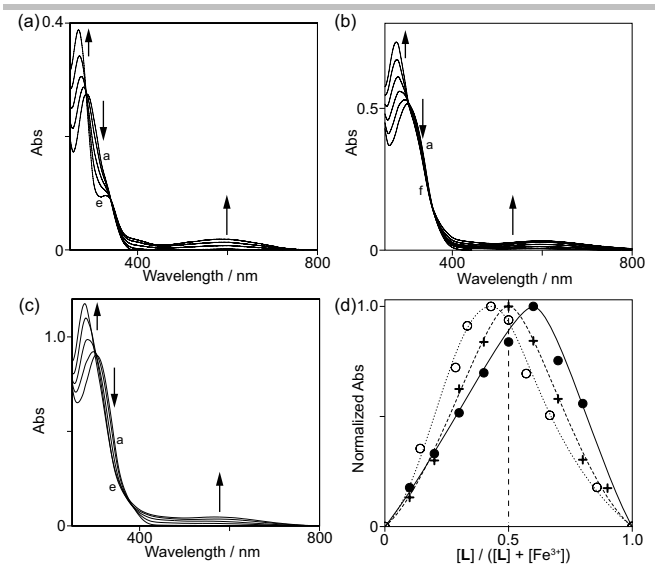

Figure 2. Changes in the UV/vis absorption spectra of (a) K_2**L1** (2.0 × 10^{-5} mol L^{-1}) with $Fe(acac)_3$ (a–e: 0.0, 0.34, 0.68, 1.02, 1.34 × 10^{-5} mol L^{-1}), (b) K_3**L2** (2.0 × 10^{-5} mol L^{-1}) with $Fe(acac)_3$ (a–f: 0.0, 0.4, 0.8, 1.2, 1.6, 2.0 × 10^{-5} mol L^{-1}), and (c) K_4**L3** (2.0 × 10^{-5} mol L^{-1}) with $Fe(acac)_3$ (a–e: 0.0, 0.67, 1.3, 2.0, 2.7 × 10^{-5} mol L^{-1}) in methanol at 298 K. (d) Job plots of K_2**L1** (filled circles), K_3**L2** (crosses), and K_4**L3** (open circles) with $Fe(acac)_3$ in methanol. The total concentration of the ligands and [$Fe(acac)_3$] was maintained at 2 × 10^{-5} mol L^{-1}.

To gain detailed structural insights into metallohelicates **1a**–**3a** using ^{1}H NMR spectroscopy, Ga(III) ion was employed instead of Fe(III) ion in order to avoid the paramagnetic line broadening. Figure 3 displays the sharp ^{1}H NMR spectra of helicates **1b** and **3b** at 323 K, while **2b** gave rise to an ill-defined broad NMR spectrum. ^{1}H NMR spectrum of **1b** showed the presence of a single compound in the solution. The aromatic protons Ha–Hf appeared as fairly sharp signals, showing the signatures of a D_{3h}-symmetric structure due to the rapid exchange between the *Δ*,*Δ*-form and the *Λ*,*Λ*-form.[13a] The ^{1}H NMR spectrum was temperature-dependent. Upon cooling the solution, the interconversion of the *Δ*,*Δ*- and *Λ*,*Λ*-forms became slow on the NMR timescale, and **1b** exhibited two sets of the calixarene aromatic protons Hd–Hf at 233 K. The energetic barrier of 52.1 kJ mol^{-1} was determined at the coalescence temperature (T_c) of 273 K for Hd (Fig. S30). The ^{1}H NMR spectrum of metallohelicate **3b** at 323 K also suggests the D_{3h} symmetry of the structure. Although the catechol protons Ha–Hc, Hi, and Hj were well-resolved and sharp at 323 K, the calixarene aromatic protons Hd, Hf, and Hh were fairly broadened, implying that the interconversion process between the helical *Δ*,*Δ*,*Δ*,*Δ*-form and the *Λ*,*Λ*,*Λ*,*Λ*-form is slower than that of **1b**. Cooling the solution led to the two sets of the calixarene aromatic protons Hd–Hh and Hk–Hm below 300 K. The energetic barrier of 64.5 kJ mol^{-1} was determined at T_c of 293 K for Hd (Fig. S32). The activation energy of **3b** is only 1.2 times as large as that of **1b** although the number of the metal cores for **3b** is the double of those for **1b**. These findings suggest that each tris(catecholato)gallium(III) core in **3b** may be fairly independent in the interconversion process between the *Δ*-form and *Λ*-form, as reported by Raymond and co-workers.[13d]

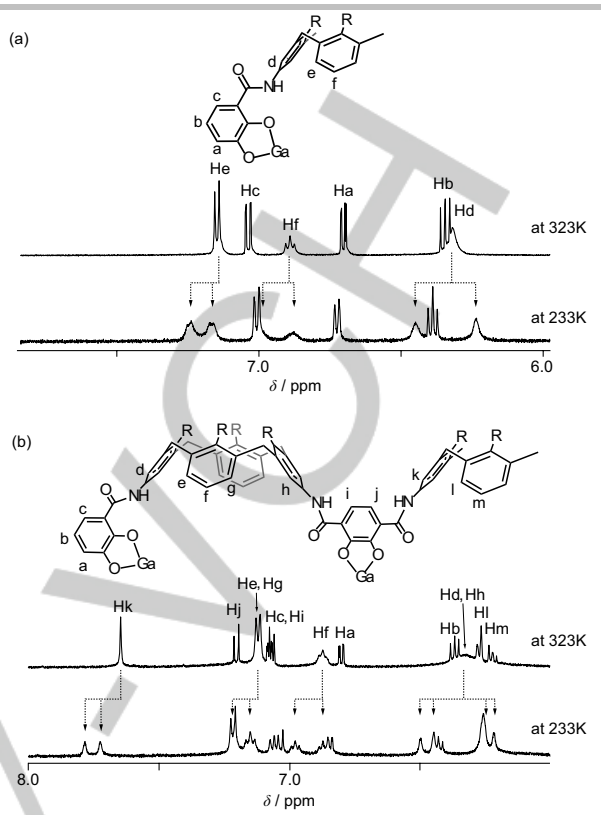

Figure 3. ^{1}H NMR spectra of (a) **1b** and (b) **3b** in methanol-d_4.

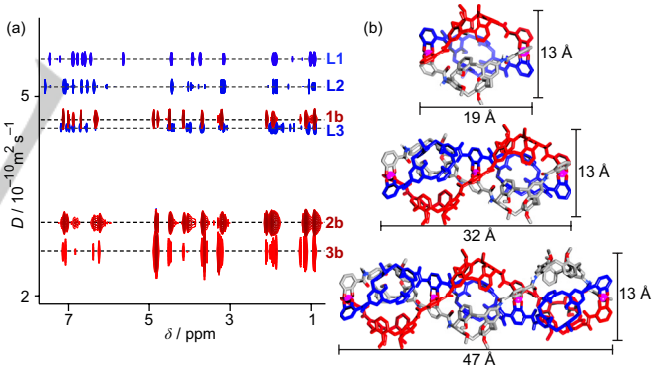

Figure 4. (a) 2D DOSY spectra of **L1**, **L2**, **L3**, **1b**, **2b**, and **3b** in methanol-d_4 at ambient temperature. (b) Energy minimized structures of (*M*)-**1b**, (*M*)-**2b**, and (*M*)-**3b**. Hydrogen atoms are omitted for clarity.

Diffusion-ordered NMR spectroscopy (DOSY) is known to be useful for the examination of the size of molecular assemblies in solution. The use of the DOSY technique allows us to obtain molecular diffusion coefficients that estimate the hydrodynamic radii of either a molecule or a molecular assembly.[23] Figure 4a shows 2D DOSY spectra of ligands **L1**–**L3** and metallohelicates **1b**–**3b**. One sets of the signals was observed, showing that the self-assembly of the ligands with the Ga(III) ions resulted in the uniform complexes without any polymeric aggregates.

10.1002/chem.201800997

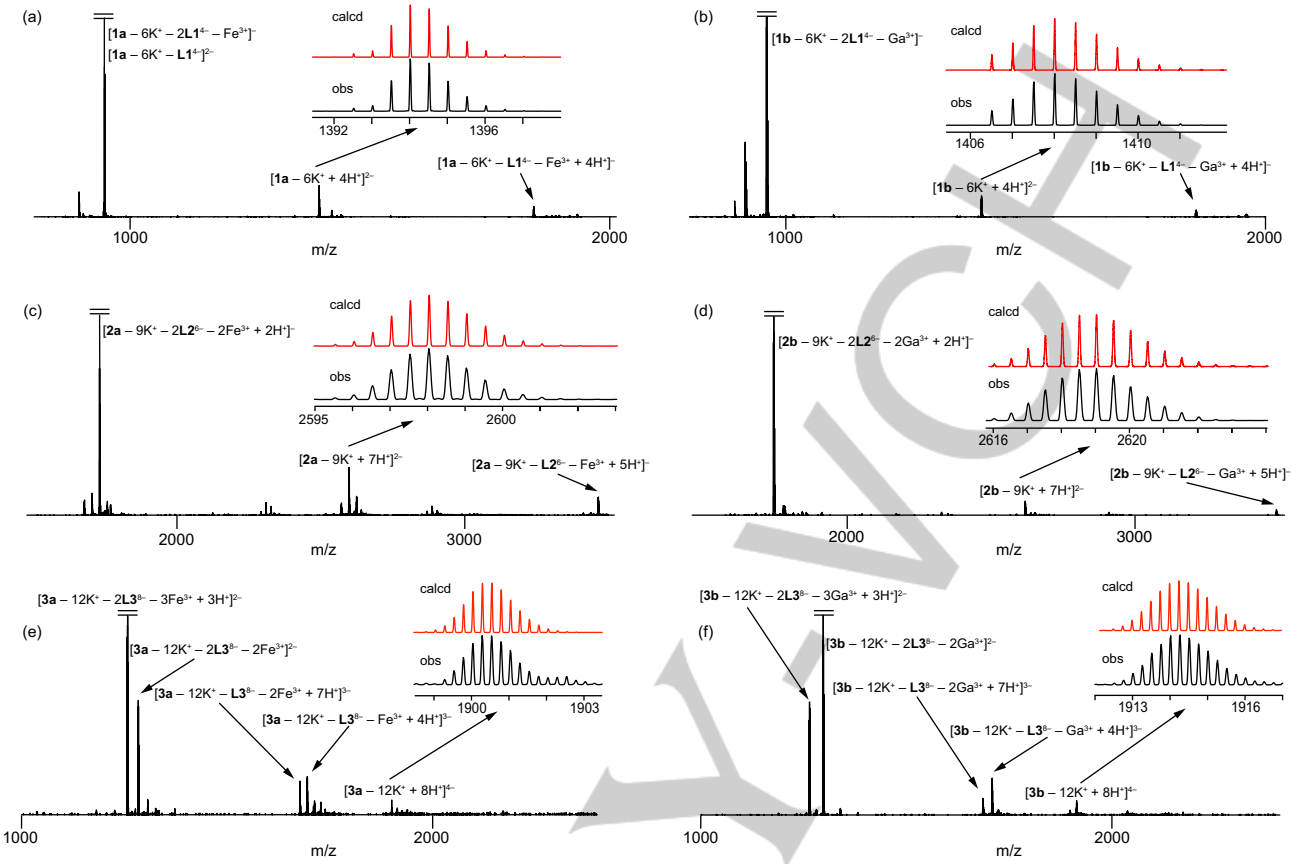

Figure 5. ESI-MS spectra of (a) **1a**, (b) **1b**, (c) **2a**, (d) **2b**, (e) **3a**, and (f) **3b**. Insets indicate the (red) calculated and (black) observed isotopic distributions.

Diffusion coefficients of 4.07(2) × 10^{-10}, 3.06(3) × 10^{-10}, and 2.366(6) × 10^{-10} m^2 s^{-1} calculated for **1b**, **2b**, and **3b** at 293 K are obviously smaller than those of 6.64(6) × 10^{-10}, 5.82(8) × 10^{-10}, and 3.95(6) × 10^{-10} m^2 s^{-1} for **L1**, **L2**, and **L3**. These findings confirm that metallohelicates **1b**, **2b**, and **3b** are large compared to the corresponding ligands. Assuming that all the helicates are spherical, the hydrodynamic radii (r_h) of the metallohelicates **1b**, **2b**, and **3b** were calculated from the diffusion coefficients by the Stokes-Einstein equation, $D = k_B T/(6\pi\eta r_h)$ (k_B is the Boltzmann constant and η is the viscosity of methanol at 293 K). The hydrodynamic radii (r_h) of 8.9, 11.8, and 15.3 Å for **1b**, **2b**, and **3b** were proportional to the number of the calixarene cores. However, the hard sphere approximation may be valid only for helicate **1b**, whereas helicates **2b** and **3b** are obviously non-spherical. The modified Storks-Einstein equation, $D = k_B T/(cf(p)\pi\eta r_h)$ (c is a size correlation factor and $f(p)$ is the shape correlation factor) takes into account deviation from the hard sphere approximation.[24] When the helicates are considered as prolate ellipsoids, their diffusions can provide detailed insights into ellipsoidal dimensions with the shape correction factors $f(p)$, resulting in the geometrical factor p, which is a ratio of the semi-major axis a and the semi-minor axis b (Table 1).[25]

Table 1. Diffusion coefficients (D), hydrodynamic radii (r_h), equivalent radii (r_{eq}), shape factors ($f(p)$), geometrical factors (p), and ratios of semi-major axes (a) and semi-minor axes (b) of the optimized structures **1b**, **2b**, and **3b**.

Helicates	D / 10^{-10} m^2 s^{-1}	r_h / Å	r_{eq} / Å	$f(p)$	p	a/b
1b	4.07(2)	9.08	8.98	0.99	1.4	1.5
2b	3.06(3)	12.0	11.1	0.93	2.4	2.5
3b	2.366(6)	15.4	12.7	0.83	4.4	3.6

Molecular mechanics calculation of a supramolecular complex enables the visualization of its size, shape, and dimensions. For greater insight, the structures of metallohelicates **1b**, **2b**, and **3b** were calculated by MacroModel V9.1 using the AMBER* force field.[26] Figure 4b displays the energy-minimized structures of **1b**, **2b**, and **3b**, which are obviously cigar-like ellipsoids. The stable structures of the triple-stranded metallohelicates possess 3-fold rotational axes through the Ga^{3+} centers. Each monomer unit was twisted with the angle of approximately 155°, giving rise to the pseudo D_3-symmetric triple-stranded structures. Each metal ion adopts the Δ-configuration in the (P)-conformers and the Λ-configuration in the (M)-conformers. Base on the molecular volumes of the optimized structures, the

10.1002/chem.201800997

spherical equivalent radii (r_{eq}) were calculated (Table 1). For all the helicates, r_{eq}s are slightly smaller than r_hs, which yields shape factors ($f(p)$) of 0.99–0.83, and the geometrical factors (p) of 1.4–4.4 for **1b**, **2b**, and **3b**. The molecular dimensions of **1b**, **2b**, and **3b** were shown in Figure 4b. The ratios of semi-major and semi-minor axes for the optimized structures are in fair agreement with the geometrical factors (p). Accordingly, helicates **1b**, **2b**, and **3b** behave in solution as cigar-like ellipsoids with dimensions very similar to those found in the optimized structures.

Mass spectrometry provides evidence for the formation of the metallohelicates in the gas phase.[27] Metallohelicates **1a**,**b**, **2a**,**b**, and **3a**,**b** can be negatively charged upon being infused into the mass analyzer. The ESI-MS spectra of **1a** and **1b** gave rise to the most abundant peaks of 1394.02 and 1408.01, corresponding to $[\mathbf{1a} - 6K^+ + 4H^+]^{2-}$ and $[\mathbf{1b} - 6K^+ + 4H^+]^{2-}$, respectively. The ligand fragmentation occurred easily in the gas phase, resulting in $[\mathbf{1a},\mathbf{b} - 6K^+ - \mathbf{L1}^{4-} - M^{3+} + 4H^+]^-$ and $[\mathbf{1a},\mathbf{b} - 6K^+ - 2\mathbf{L1}^{4-} - M^{3+}]^-$. Helicates **2a** and **2b** were successfully ionized to produce the divalent molecular ions of $[\mathbf{2a} - 9K^+ + 7H^+]^{2-}$ and $[\mathbf{2b} - 9K^+ + 7H^+]^{2-}$, emerging at 2598.03 and 2619.02, respectively, with a certain amount of the fragment ions of $[\mathbf{2a},\mathbf{b} - 9K^+ - \mathbf{L2}^{6-} - M^{3+} + 5H^+]^-$ and $[\mathbf{2a},\mathbf{b} - 9K^+ - 2\mathbf{L2}^{6-} - 2M^{3+} + 2H^+]^-$. In the ESI-MS spectra of **3a** and **3b**, the tetravalent molecular ions of **3a** and **3b** were successfully detected as weak peaks of 1900.52 and 1914.26, corresponding to $[\mathbf{3a} - 12K^+ + 8H]^{4-}$ and $[\mathbf{3b} - 12K^+ + 8H]^{4-}$, respectively. However, many ligand-fragmented ions of $[\mathbf{3a},\mathbf{b} - 12K^+ - \mathbf{L3}^{8-} - M^{3+} + 4H^+]^{3-}$, $[\mathbf{3a},\mathbf{b} - 12K^+ - \mathbf{L3}^{8-} - 2M^{3+} + 7H^+]^{3-}$, $[\mathbf{3a},\mathbf{b} - 12K^+ - 2\mathbf{L3}^{8-} - 2M^{3+}]^{2-}$, and $[\mathbf{3a},\mathbf{b} - 12K^+ - 2\mathbf{L3}^{8-} - 3M^{3+} + 3H^+]^{2-}$ were simultaneously detected, most likely due to the highly charged nature of the molecular ions. All ESI-MS measurements provided the well-resolved peaks of the molecular ions and their ligand-fragmented ions which were in good agreement with their calculated isotope distributions, confirming the formation of the metallohelicates in the gas phase. The ligand-fragmented ions observed in all MS spectra suggest that the metallohelicates are most likely labile due to the reversible coordination bonds of the tris(catecholato)iron or the gallium complex.

Guest Complexation

To examine the formation of host-guest complexes, the methyl pyridinium guests **4**–**7** bearing amino acid esters were employed. ^{1}H NMR titration experiment of (*R*)-**4** were carried out with **1b** (Figure 6a). Upon the addition of **1b**, the aromatic protons Hb, Hc, He, and the two methyl protons Ha, Hd of the pyridine ring exhibited upfield shifts, while no upfield shift of the methyl ester group was observed. These results indicate that the *N*-methyl pyridinium ring was selectively accommodated within the cavity of **1b**, experiencing the shielding effect of the aromatic rings of the three calix[4]arene units, and the ester methyl group remained outside the cavity. The acidic N^+–CH_3 protons of (*R*)-**4** should participate in the host-guest complexation through the intermolecular CH/π interaction in the π–basic cavity. To confirm the contribution of the CH/π interaction, the reference guest **8,** which does not possess any positively charged methyl moieties on the aromatic rings, was titrated with **1b** instead of guest (*R*)-**4**. No change was observed in the chemical shifts of their protons; therefore, the intermolecular CH/π interaction of the acidic N^+–CH_3 protons within the cavity of **1b** primarily drives the host-guest complexation. The multiple guest-binding cavities of **2b** and **3b** encapsulated the methyl pyridinium ring of (*R*)-**4** (Figure 6b). The pyridinium protons Hb,c shifted upfield in the presence of **1b**, **2b**, and **3b**, while the upfield shifts for the methyl ester proton Hf were negligible.

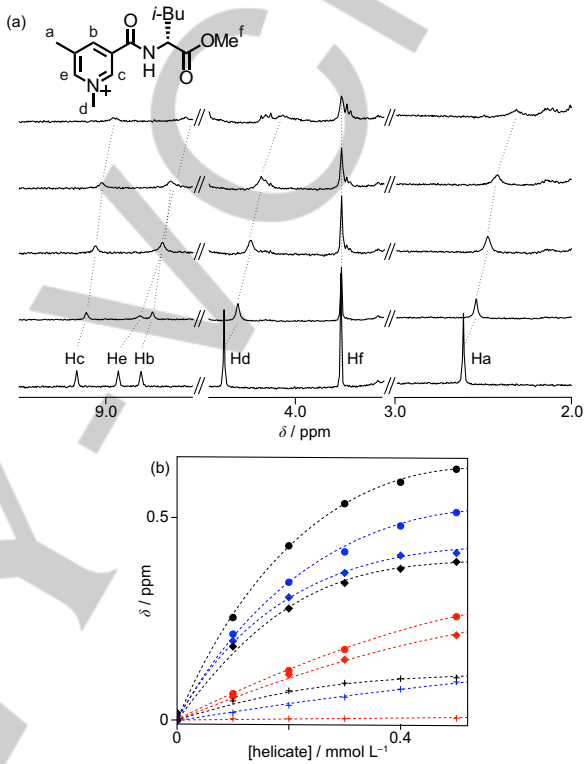

Figure 6. (a) ^{1}H NMR of guest (*R*)-**4** (1.0×10^{-3} mol L^{-1}) in the presence of **1b** (from bottom to top: 0, 1.0, 2.0, 3.0, 5.0×10^{-4} mol L^{-1}) at 298 K in methanol-d_4. (b) Chemical shift changes of protons Hb (filled circles), Hc (filled rhombuses), and Hf (crosses) of (*R*)-**4** (1.0×10^{-3} mol L^{-1}) in the presence of helicates **1b** (red), **2b** (blue), and **3b** (black).

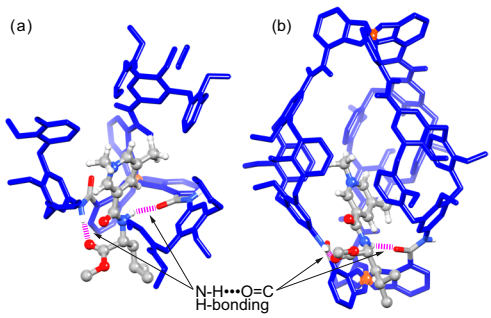

Figure 7. (a) Top view and (b) side view of the calculated structure of the host-guest complex (*R*)-**4**⊂**1b**.

Molecular mechanics calculations are helpful for understanding the intermolecular association of the host-guest

complex (*R*)-**4**⊂**1b**. The conformational search was carried out using low-mode search algorithm[28] to generate 1000 initial geometries, which were then optimized using the AMBER* force field. Two low-energy host-guest structures with similar characteristics are found to be within 12 kJ mol^{-1} of each other. The most stable conformation is shown in Figure 7. The *N*-methyl group stays in one of the calixarene cavities, which evidences the presence of the CH/π interaction. The guest amide N-H is hydrogen-bonded to one of the amide carbonyl group of the host, and the ester carbonyl group of the guest is directed at the N-H proton of the host to form the hydrogen bond. These attractive intermolecular CH/π and hydrogen-bonding interactions most likely drive the intermolecular association between **1b** and the cationic guests. In addition, the stereogenic carbon of the guest is located on the catechol ring. This close contact of the stereogenic carbon to the stereogenic metal center of **1b** most likely drives the one-handed helical structure of **1b**.

Determination of Binding Constants

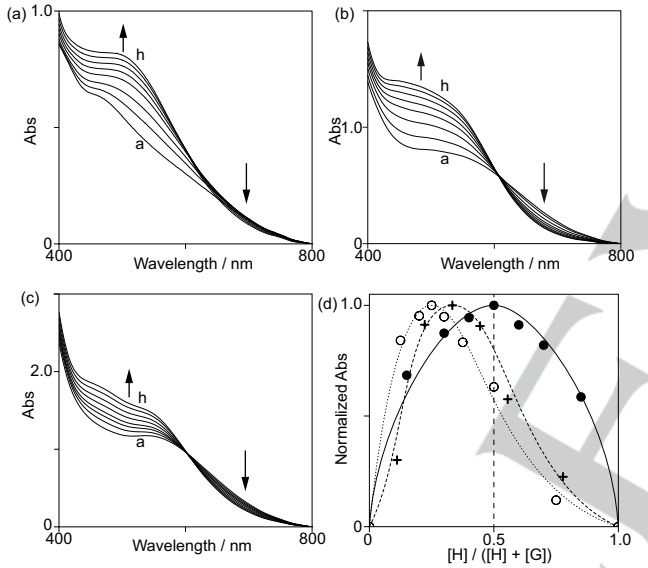

Figure 8. UV/vis absorption spectra of (a) **1a** (1.0 × 10^{-4} mol L^{-1}), (b) **2a** (1.0 × 10^{-4} mol L^{-1}), and (c) **3a** (1.0 × 10^{-4} mol L^{-1}) upon the addition of (*R*)-**4** (a–h: (a) 0.0, 0.98, 1.9, 3.3, 4.6, 6.1, 8.0, 10.0 × 10^{-4} mol L^{-1}; (b) 0.0, 0.98, 1.9, 2.8, 3.7, 5.0, 6.9, 10.0 × 10^{-4} mol L^{-1}; (c) 0.0, 1.9, 3.2, 4.1, 5.3, 6.5, 8.0, 10.0 × 10^{-4} mol L^{-1}) in methanol at 298 K. (d) Job plots of **1a** (filled circles), **2a** (crosses), and **3a** (open circles) with (*R*)-**4** in methanol. The total concentration of the helicates and (*R*)-**4** was maintained to be 1.0 × 10^{-4} mol L^{-1}.

To discuss the cooperative effects for the conformationally coupled multiple cavities, the guest binding abilities of **1a**, **2a**, and **3a** were evaluated using UV/vis absorption spectroscopy. The tris(catecholato)iron(III) cores provide the LMCT band in the visible region, which was quite sensitive for guest binding (Figures 8a,b,c). When (*R*)-**4** was added into the solutions of **1a**, **2a**, and **3a**, the broad band at approximately 700 nm gradually decreased, and new bands at approximately 500 nm emerged with isosbestic points at approximately 600 nm. The stoichiometries for the host-guest complexes of **1a**, **2a**, and **3a** with (*R*)-**4** were determined using Job plots (Figure 8d). The host-guest ratios of 1:1, 1:2, and 1:3 for **1a**, **2a**, and **3a**, respectively, are perfectly matched with the number of the guest binding cavities of the helicates; thereby, all cavities of the metallohelicates are capable of encapsulating the guest molecules. The experimental spectra were elaborated with the HypSpec program,[29] and subjected to a non-linear global analysis by applying 1:1 and 1:2 host-guest models of binding to determine the association constants for **1a** and **2a**. The binding constants of **1a** and **2a** for guests **4**–**7** are shown in Table 2. Upon the application of the 1:3 host-guest model of binding for **3a**, the binding constants (K_1–K_3) were not directly obtained. A non-linear global analysis was repeatedly carried out with the arbitrary K_1 values estimated based on the results for **1a** and **2a** until the residual errors reached the smallest possible values.

Metallohelicates **1a**, **2a**, and **3a** encapsulate guests **4**–**7** bearing the amino acid side chains with the large binding constants in the range of 10^3–10^4 L mol^{-1}. The first guest binding into the cavities of the helicates was gradually facilitated from **1a** to **3a**, most likely implying that the cavities become structurally preorganized as increasing the number of the metal centers. The alkyl substituents of the amino acid side chains strongly influenced the guest binding. The steric interaction of the benzyl group for **5** is likely to be repulsive to the exterior of the cavities (entry 7 and 10 versus 4; 8 and 11 versus 5; 9 and 12 versus 6). By contrast, the *iso*-butyl group may result in the attractive interaction to the aromatic exterior of the helicates (entry 2 versus 8 and 11; 3 versus 9 and 12).

Table 2. Binding constants of metallohelicates **1a**, **2a**, and **3a** with (*R*)-**4**, (*R*)-**5**, (*R*)-**6**, and **7**.

entry	Guest	Host	K_1 / L mol^{-1}	K_2 / L mol^{-1}	K_3 / L mol^{-1}
1	(*R*)-**4**	**1a**	2.99(2) × 10^3	—	—
2		**2a**	7.48(8) × 10^3	8.4(1) × 10^3	—
3		**3a**	7.94 × 10^{3a}	9.15(5) × 10^3	5.04(3) × 10^3
4	(*R*)-**5**	**1a**	1.32(1) × 10^3	—	—
5		**2a**	1.72(3) × 10^3	2.45(5) × 10^3	—
6		**3a**	2.34 × 10^{3a}	5.1(1) × 10^3	5.8(1) × 10^3
7	(*R*)-**6**	**1a**	3.58(4) × 10^3	—	—
8		**2a**	4.00(5) × 10^3	6.9(1) × 10^3	—
9		**3a**	4.12 × 10^{3a}	4.6(1) × 10^3	1.4(1) × 10^4
10	**7**	**1a**	5.11(3) × 10^3	—	—
11		**2a**	3.10(7) × 10^3	2.70(8) × 10^3	—
12		**3a**	6.31 × 10^{3a}	5.1(1) × 10^3	2.31(6) × 10^4

[a]Estimated based on standard errors given by the analysis.

Cooperativity in Guest Binding

The conformationally coupled multiple guest binding sites of a multitopic host molecule often show cooperativity in their multiple guest association.[30] At the molecular level, the cooperativity in the multiple guest binding is described by the interaction

parameters α defined by the equations: $\alpha_{12} = 4K_2/K_1$ and $\alpha_{12} = 3K_2/K_1$, $\alpha_{23} = 3K_3/K_2$ for the 1:2 host-guest system and the 1:3 host-guest system, respectively. To evaluate the cooperative effect in the multiple host-guest complexations of helicates **2a** and **3a**, the interaction parameters (α) for the multiple guest binding were calculated (Table 3). The interaction parameters α_{12} and α_{23} of **2a** and **3a** are greater than unity, indicating that positive cooperative effects are present in the encapsulation of the second and the third guests. Therefore, the conformationally coupled two or three binding sites sterically communicate with each other through the tris(catecholato)iron(III) cores; that is, the first or second guest binding information is effectively transferred, and preorganizes the remaining binding sites. Then, the successive guests are facilitated to become accessible for encapsulation into the remaining cavities.

Table 3. Interaction parameter α of helicates **2a** and **3a** for (*R*)-**4**, (*R*)-**5**, (*R*)-**6**, and **7**.

	2a	**3a**	
Guests	α_{12}	α_{12}	α_{23}
(*R*)-**4**	4.5	3.5	1.7
(*R*)-**5**	5.7	6.5	3.4
(*R*)-**6**	6.9	3.4	9.0
7	3.5	2.4	13.7

Chiral Induction

Helicates **1a**, **2a**, and **3a** are D_3-symmetric due to the lack of a mirror plane. The (*P*)- and (*M*)-helical forms exist as racemic mixtures in solution. The labile nature of the tris(catecholato)iron(III) cores permits the dynamic interconversion between the (*P*)- and (*M*)-enantiomeric forms. When a chiral guest is encapsulated, the chiral cavities recognize the shape of the chiral guest, giving rise to an energy difference between the diastereomeric complexes. Circular dichroism (CD) spectroscopy was informative for gaining an insight into the stereoselection of the diastereomeric complexes with the chiral guests **4**–**6** (Figure 9). Induced CD emerged when the optically active (*R*)- and (*S*)-**4** were encapsulated within the cavities into the solution of the metallohelicates (Figure 9a). The addition of (*R*)-**4** in the solutions of **1a** resulted in the induced plus-to-minus bisignate CD signals at 574 and at 446 nm, corresponding to the LMCT band of the tris(catecholato)iron(III) core. The CD spectra with (*R*)-**4** and (*S*)-**4** show a mirror-image relationship with respect to the line of $\Delta\varepsilon = 0$. The signal intensities at approximately 446 nm were dependent on the number of the guest binding cavities, indicating that the chiral guest complexation within the dissymmetric cavities resulted in an energy difference between the (*P*)- and (*M*)-conformation and biased the population. Raymond and co-workers reported that the absolute stereochemistry of tris(catecholato)iron(III) was determined using CD spectroscopy.[31] The plus-to-minus cotton effects at the LMCT band correspond to the *Λ*-configuration of the metal cores in the helicates possessing the (*M*)-conformation. (*R*)-**5** and (*R*)-**6** also induced the plus-to-minus cotton effects of **1a**, **2a** and **3a**; therefore, the stereogenic centers of the amino acid groups determined the left-handed helical sense of the host-guest complex.

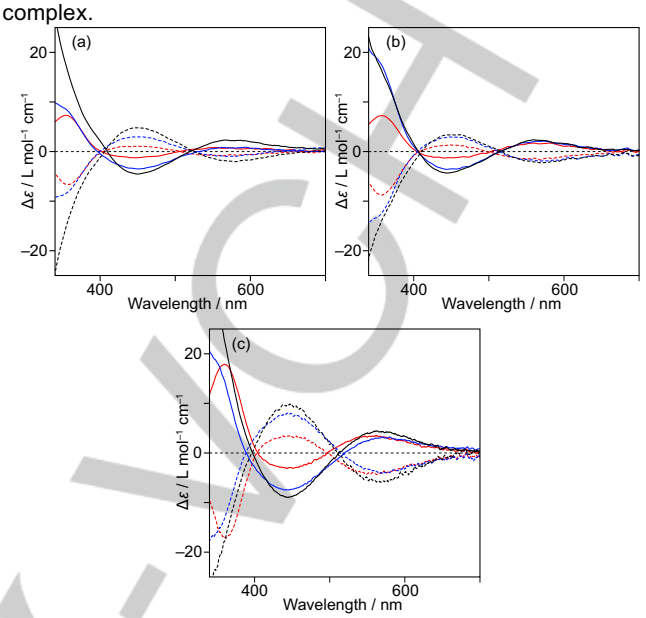

Figure 9. CD spectra of **1a** (red), **2a** (blue), and **3a** (black) (a) with (*R*)-**4** (solid line) and (*S*)-**4** (dashed line), (b) with (*R*)-**5** (solid line) and (*S*)-**5** (dashed line), and (c) with (*R*)-**6** (solid line) and (*S*)-**6** (dashed line) in methanol at 298 K. [Helicates] = 3.0×10^{-5} mol L^{-1} and [Guests] = 3.0×10^{-3} mol L^{-1}.

Majority-rules Effect

Two chiral amplification mechanisms are possible in supramolecular assemblies: the first is the sergeants-and-soldiers principle, and the second is the majority-rules principle.[32] The latter characterizes a non-linear response in chirality for the assemblies consisting of both enantiomers of chiral monomers. Small excess of one of the enantiomers results in a chiral response in a non-linear fashion.[33],[34] The cooperativity of the conformationally coupled guest binding cavities of **2a** and **3a** are already established in the guest binding; therefore, majority rules principle can be operative in the chiral guest recognition for **2a** and **3a**. Figure 10a shows the CD spectra of **2a** upon the variation of the enantiomeric excess (*ee*) of **6**. To confirm the cooperative effect on the molecular recognition, the induced circular dichroism (ICD) intensities at the LMCT bands versus the *ee* of guests **4**–**6** were plotted (Figures 10b,c,d). The complexation of **1a** with chiral guests **4**–**6** gave rise to the good linear correlation between the ICD intensities and the *ee* of the guests. In contrast, the complexation of the chiral guests **4**–**6** to the multiple guest binding cavities of **2a** and **3a** showed a remarkable deviation from linearity, indicating that the enantiomers in excess had a disproportionate impact on the helicity of the metallohelicates.[19] The deviation was maximized when the guests were encapsulated within **3a** over **2a**, suggesting that the cavities of **3a** are more preorganized in a helical manner than those of **2a**. The majority-rules effects are influenced by the steric bulkiness of the amino acid side chains. The complexation of **4** to **2a** and **3a** showed smaller deviations than the complexations of **5** and **6**. Accordingly, the amino acid

side chains most likely generate the steric interaction to the stereogenic metal centers, determining the absolute helical sense of the metallohelicates.

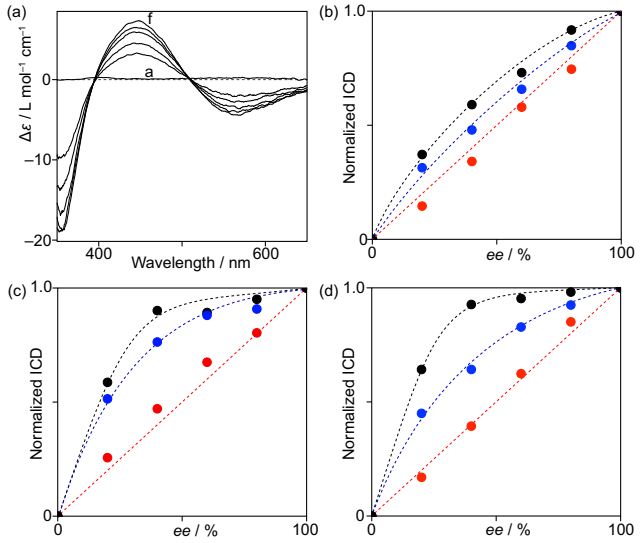

Figure 10. (a) CD spectra of **2a** (1.0×10^{-4} mol L^{-1}) in the presence of mixtures $[(S)\text{-}\mathbf{6}]_x + [(R)\text{-}\mathbf{6}]_{1-x}$ (1.0×10^{-2} mol L^{-1}) (a–f: X = 0.5, 0.60, 0.70, 0.80, 0.90, 1.00) in methanol at 298 K. (b)–(d) Plots of normalized ICD intensities at the LMCT bands of **1a** (red circle), **2a** (blue circle), and **3a** (black circle) versus *ee* of (b) **4,** (c) **5,** and (d) **6**. [Helicates] = 1.0×10^{-4} mol L^{-1} and [Guests] = 1.0×10^{-2} mol L^{-1}.

Conclusions

In conclusion, we have demonstrated that the triple-stranded metallohelicates can be developed through the self-organization of the trivalent metal ions and the multidentate bridging ligands. The multiple guest-binding cavities are conformationally coupled; therefore, a first guest binding preorganizes the rest of the binding cavities in the multiple cavities; as a result, large positive cooperative effects are manifested in the guest binding. The chiral guest complexation within the multiple guest-binding cavities determines the helical sense of the metallohelicates, directed by the stereogenic center of the amino acid. The chiral guest complexation to the metallohelicates gives rise to the non-linear relationships in the stereoselection for the helical direction, which are the so-called majority-rules effects. Accordingly, the induced chirality on a monomer unit is communicated to the other units through the strands, modulating the internal spaces in such a way that the second and the third guests are easily accessible for the remaining cavities. These findings offer a facile synthetic strategy for readily preparing optically active multiple-stranded organizations with controlled helicity.

Acknowledgements

This work was supported by Grants-in-Aid for Scientific Research, JSPS KAKENHI Grant Numbers JP15H03817 and JP15KT0145, and by Grants-in-Aid for Scientific Research on Innovative Areas, JSPS KAKENHI Grant Numbers JP15H00946 (Stimuli-responsive Chemical Species), JP15H00752 (New Polymeric Materials Based on Element-Blocks), JP17H05375 (Coordination Asymmetry), and JP17H05159 (π-Figuration). We also acknowledge the Futaba Electronics Memorial Foundation.

Keywords: helicate • supramolecular chemistry • allostery • majority-rules effect • calixarene

[1] R. A. Hegstrom and D. K. Kondepudi, *Sci. Am.* **1990**, *262*, 108-115.
[2] A. Klug, *Angew. Chem. Int. Ed. Engl.* **1983**, *22*, 565-582.
[3] K. C. Holmes, D. Popp, W. Gebhard and W. Kabsch, *Nature* **1990**, *347*, 44-49.
[4] J. D. Watson and F. H. C. Crick, *Nature* **1953**, *171*, 737-738.
[5] L. Pauling, R. B. Corey and H. R. Branson, *Proc. Natl. Acad. Sci. USA* **1951**, *37*, 205-211.
[6] a) M. Liu, L. Zhang and T. Wang, *Chem. Rev.* **2015**, *115*, 7304-7397; b) E. Yashima, N. Ousaka, D. Taura, K. Shimomura, T. Ikai and K. Maeda, *Chem. Rev.* **2016**, *116*, 13752-13990.
[7] a) J. M. Lehn, *Supramolecular Chemistry: Concepts and Perspectives*, VCH, Weinheim, **1995**, p; b) M. A. Mateos-Timoneda, M. Crego-Calama and D. N. Reinhoudt, *Chem. Soc. Rev.* **2004**, *33*, 363-372; c) E. Yashima, K. Maeda and Y. Furusho, *Acc. Chem. Res.* **2008**, *41*, 1166-1180; d) Q. Jin, L. Zhang, H. Cao, T. Wang, X. Zhu, J. Jiang and M. Liu, *Langmuir* **2011**, *27*, 13847-13853; e) M. M. Safont-Sempere, G. Fernández and F. Würthner, *Chem. Rev.* **2011**, *111*, 5784-5814; f) J. Kumar, T. Nakashima, H. Tsumatori and T. Kawai, *J. Phys. Chem. Lett.* **2014**, *5*, 316-321.
[8] a) N. Kimizuka, T. Kawasaki, K. Hirata and T. Kunitake, *J. Am. Chem. Soc.* **1995**, *117*, 6360-6361; b) J. H. K. K. Hirschberg, L. Brunsveld, A. Ramzi, J. A. J. M. Vekemans, R. P. Sijbesma and E. W. Meijer, *Nature* **2000**, *407*, 167-170; c) M. Reggelin, M. Schultz and M. Holbach, *Angew. Chem. Int. Ed.* **2002**, *41*, 1614-1617; d) P. Jonkheijm, F. J. M. Hoeben, R. Kleppinger, J. van Herrikhuyzen, A. P. H. J. Schenning and E. W. Meijer, *J. Am. Chem. Soc.* **2003**, *125*, 15941-15949; e) M. M. J. Smulders, A. P. H. J. Schenning and E. W. Meijer, *J. Am. Chem. Soc.* **2008**, *130*, 606-611; f) T. Yamamoto and M. Suginome, *Angew. Chem. Int. Ed.* **2009**, *48*, 539-542; g) S. Yagai, H. Aonuma, Y. Kikkawa, S. Kubota, T. Karatsu, A. Kitamura, S. Mahesh and A. Ajayaghosh, *Chem. Eur. J.* **2010**, *16*, 8652-8661; h) F. Würthner, T. E. Kaiser and C. R. Saha-Möller, *Angew. Chem. Int. Ed.* **2011**, *50*, 3376-3410; i) R. P. Megens and G. Roelfes, *Chem. Eur. J.* **2011**, *17*, 8514-8523; j) P. A. Korevaar, S. J. George, A. J. Markvoort, M. M. J. Smulders, P. A. J. Hilbers, A. P. H. J. Schenning, T. F. A. De Greef and E. W. Meijer, *Nature* **2012**, *481*, 492-496; k) T. Miyabe, H. Iida, A. Ohnishi and E. Yashima, *Chem. Sci.* **2012**, *3*, 863-867; l) S. I. Stupp and L. C. Palmer, *Chem. Mater.* **2014**, *26*, 507-518; m) Y. Akai, L. Konnert, T. Yamamoto and M. Suginome, *Chem. Commun.* **2015**, *51*, 7211-7214; n) H. Wang, N. Li, Z. Yan, J. Zhang and X. Wan, *RSC Adv.* **2015**, *5*, 2882-2890; o) Y. Yoshinaga, T. Yamamoto and M. Suginome, *ACS Macro Lett.* **2017**, *6*, 705-710.
[9] a) D. M. Bassani, J.-M. Lehn, G. Baum and D. Fenske, *Angew. Chem. Int. Ed. Engl.* **1997**, *36*, 1845-1847; b) O. Mamula, A. von Zelewsky, T. Bark and G. Bernardinelli, *Angew. Chem. Int. Ed.* **1999**, *38*, 2945-2948; c) V. Berl, I. Huc, R. G. Khoury and J.-M. Lehn, *Chem. Eur. J.* **2001**, *7*, 2810-2820; d) X.-M. Chen and G.-F. Liu, *Chem. Eur. J.* **2002**, *8*, 4811-4817; e) Y. Tanaka, H. Katagiri, Y. Furusho and E. Yashima, *Angew. Chem. Int. Ed.* **2005**, *44*, 3867-3870; f) H. Goto, H. Katagiri, Y. Furusho and E. Yashima, *J. Am. Chem. Soc.* **2006**, *128*, 7176-7178; g) D. Haldar and C. Schmuck, *Chem. Soc. Rev.* **2009**, *38*, 363-371; h) S. Li, C. Jia, B. Wu, Q. Luo, X. Huang, Z. Yang, Q.-S. Li and X.-J. Yang, *Angew. Chem. Int. Ed.* **2011**, *50*, 5721-5724; i) B. Wu, S. Li, Y. Lei, H. Hu, N. de Sousa Amadeu, C. Janiak, J. S. Mathieson, D.-L. Long, L. Cronin and X.-J. Yang, *Chem. Eur. J.* **2015**, *21*, 2588-2593; j) C. Jia, W. Zuo, D. Yang, Y.

Chen, L. Cao, R. Custelcean, J. Hostaš, P. Hobza, R. Glaser, Y.-Y. Wang, X.-J. Yang and B. Wu, *Nat. Commun.* **2017**, *8*.

[10] a) J.-M. Lehn, A. Rigault, J. Siegel, J. Harrowfield, B. Chevrier and D. Moras, *Proc. Natl. Acad. Sci. USA* **1987**, *84*, 2565-2569; b) A. Pfeil and J.-M. Lehn, *J. Chem. Soc., Chem. Commun.* **1992**, 838-840; c) B. Hasenknopf, J.-M. Lehn, G. Baum and D. Fenske, *Proc. Natl. Acad. Sci. USA* **1996**, *93*, 1397-1400; d) A. Marquis-Rigault, A. Dupont-Gervais, A. Van Dorsselaer and J.-M. Lehn, *Chem. Eur. J.* **1996**, *2*, 1395-1398; e) V. C. M. Smith and J.-M. Lehn, *Chem. Commun.* **1996**, 2733-2734; f) A. Marquis, V. Smith, J. Harrowfield, J.-M. Lehn, H. Herschbach, R. Sanvito, E. Leize-Wagner and A. Van Dorsselaer, *Chem. Eur. J.* **2006**, *12*, 5632-5641.

[11] a) C. A. Schalley, A. Lützen and M. Albrecht, *Chem. Eur. J.* **2004**, *10*, 1072-1080; b) C. R. K. Glasson, L. F. Lindoy and G. V. Meehan, *Coord. Chem. Rev.* **2008**, *252*, 940-963; c) S. E. Howson and P. Scott, *Dalton Trans.* **2011**, *40*, 10268-10277; d) M. Albrecht, *Chem. Rev.* **2001**, *101*, 3457-3497.

[12] a) E. C. Constable and R. Chotalia, *J. Chem. Soc., Chem. Commun.* **1992**, 64-66; b) C. Provent, S. Hewage, G. Brand, G. Bernardinelli, L. J. Charbonnière and A. F. Williams, *Angew. Chem. Int. Ed. Engl.* **1997**, *36*, 1287-1289; c) D. A. McMorran and P. J. Steel, *Angew. Chem. Int. Ed.* **1998**, *37*, 3295-3297; d) C. R. Rice, S. Wörl, J. C. Jeffery, R. L. Paul and M. D. Ward, *Chem. Commun.* **2000**, 1529-1530; e) P. K. Bowyer, V. C. Cook, N. Gharib-Naseri, P. A. Gugger, A. D. Rae, G. F. Swiegers, A. C. Willis, J. Zank and S. B. Wild, *Proc. Natl. Acad. Sci. USA* **2002**, *99*, 4877-4882; f) V. Maurizot, G. Linti and I. Huc, *Chem. Commun.* **2004**, 924-925; g) M. Bera, G. Aromí, W. T. Wong and D. Ray, *Chem. Commun.* **2006**, 671-673; h) W. Chen, X. Tang, W. Dou, B. Wang, L. Guo, Z. Ju and W. Liu, *Chem. Eur. J.* **2017**, *23*, 9804-9811; i) S. Naskar, C. Dalal and P. Ghosh, *Chem. Commun.* **2017**, *53*, 2487-2490; j) E. C. Constable, T. Kulke, M. Neuburger and M. Zehnder, *Chem. Commun.* **1997**, 489-490; k) J. S. Fleming, K. L. V. Mann, S. M. Couchman, J. C. Jeffery, J. A. McCleverty and M. D. Ward, *J. Chem. Soc., Dalton Trans.* **1998**, 2047-2052; l) V. Amendola, L. Fabbrizzi, L. Gianelli, C. Maggi, C. Mangano, P. Pallavicini and M. Zema, *Inorg. Chem.* **2001**, *40*, 3579-3587; m) R. Annunziata, M. Benaglia, A. Famulari and L. Raimondi, *Magn. Reson. Chem.* **2001**, *39*, 341-354; n) W. Schuh, H. Kopacka, K. Wurst and P. Peringer, *Chem. Commun.* **2001**, 2186-2187.

[13] a) B. Kersting, M. Meyer, R. E. Powers and K. N. Raymond, *J. Am. Chem. Soc.* **1996**, *118*, 7221-7222; b) B. Kersting, J. R. Telford, M. Meyer and K. N. Raymond, *J. Am. Chem. Soc.* **1996**, *118*, 5712-5721; c) D. L. Caulder and K. N. Raymond, *Angew. Chem. Int. Ed. Engl.* **1997**, *36*, 1440-1442; d) M. Meyer, B. Kersting, R. E. Powers and K. N. Raymond, *Inorg. Chem.* **1997**, *36*, 5179-5191.

[14] E. J. Enemark and T. D. P. Stack, *Angew. Chem. Int. Ed. Engl.* **1995**, *34*, 996-998.

[15] a) M. Albrecht and S. Kotila, *Angew. Chem. Int. Ed. Engl.* **1995**, *34*, 2134-2137; b) I. Janser, M. Albrecht, K. Hunger, S. Burk and K. Rissanen, *Eur. J. Inorg. Chem.* **2006**, 244-251; c) M. Albrecht, E. Isaak, H. Shigemitsu, V. Moha, G. Raabe and R. Fröhlich, *Dalton Trans.* **2014**, *43*, 14636-14643; d) D. Van Craen, M. Albrecht, G. Raabe, F. Pan and K. Rissanen, *Chem. Eur. J.* **2016**, *22*, 3255-3258.

[16] a) H. V. Huynh, C. Schulze Isfort, W. W. Seidel, T. Lügger, R. Fröhlich, O. Kataeva and F. E. Hahn, *Chem. Eur. J.* **2002**, *8*, 1327-1335; b) F. E. Hahn, C. Schulze Isfort and T. Pape, *Angew. Chem. Int. Ed.* **2004**, *43*, 4807-4810; c) C. Schulze Isfort, T. Kreickmann, T. Pape, R. Fröhlich and F. E. Hahn, *Chem. Eur. J.* **2007**, *13*, 2344-2357; d) F. E. Hahn, M. Offermann, C. Schulze Isfort, T. Pape and R. Fröhlich, *Angew. Chem. Int. Ed.* **2008**, *47*, 6794-6797.

[17] a) R. M. Yeh, M. Ziegler, D. W. Johnson, A. J. Terpin and K. N. Raymond, *Inorg. Chem.* **2001**, *40*, 2216-2217; b) R. M. Yeh and K. N. Raymond, *Inorg. Chem.* **2006**, *45*, 1130-1139.

[18] a) D. Zare, Y. Suffren, H. Nozary, A. Hauser and C. Piguet, *Angew. Chem. Int. Ed.* **2017**, *56*, 14612-14617; b) J. L. Greenfield, F. J. Rizzuto, I. Goldberga and J. R. Nitschke, *Angew. Chem. Int. Ed.* **2017**, *56*, 7541-7545; c) F. Cui, S. Li, C. Jia, J. S. Mathieson, L. Cronin, X.-J. Yang and B. Wu, *Inorg. Chem.* **2012**, *51*, 179-187; d) U. Kiehne, T. Weilandt and A. Lützen, *Org. Lett.* **2007**, *9*, 1283-1286; e) C. J. Baylies, T. Riis-Johannessen, L. P. Harding, J. C. Jeffery, R. Moon, C. R. Rice and M. Whitehead, *Angew. Chem. Int. Ed.* **2005**, *44*, 6909-6912; f) A. Lützen, M. Hapke, J. Griep-Raming, D. Haase and W. Saak, *Angew. Chem. Int. Ed.* **2002**, *41*, 2086-2089; g) M. Greenwald, D. Wessely, E. Katz, I. Willner and Y. Cohen, *J. Org. Chem.* **2000**, *65*, 1050-1058; h) N. Fatin-Rouge, S. Blanc, E. Leize, A. Van Dorsselaer, P. Baret, J.-L. Pierre and A.-M. Albrecht-Gary, *Inorg. Chem.* **2000**, *39*, 5771-5778; i) M. Greenwald, D. Wessely, I. Goldberg and Y. Cohen, *New J. Chem.* **1999**, *23*, 337-344; j) J. J. Jodry and J. Lacour, *Chem. Eur. J.* **2000**, *6*, 4297-4304; k) G. Baum, E. C. Constable, D. Fenske and T. Kulke, *Chem. Commun.* **1997**, 2043-2044.

[19] a) S.-Y. Chang, H.-Y. Jang and K.-S. Jeong, *Chem. Eur. J.* **2004**, *10*, 4358-4366; b) S. Freye, J. Hey, A. Torras-Galán, D. Stalke, R. Herbst-Irmer, M. John and G. H. Clever, *Angew. Chem. Int. Ed.* **2012**, *51*, 2191-2194; c) O. Gidron, M. Jirásek, M. Wörle and F. Diederich, *Chem. Eur. J.* **2016**, *22*, 16172-16177; d) W. J. Ramsay, T. K. Ronson, J. K. Clegg and J. R. Nitschke, *Angew. Chem. Int. Ed.* **2013**, *52*, 13439-13443.

[20] T. Haino, H. Shio, R. Takano and Y. Fukazawa, *Chem. Commun.* **2009**, 2481-2483.

[21] A. M. A. van Wageningen, E. Snip, W. Verboom, D. N. Reinhoudt and H. Boerrigter, *Liebigs Ann. Recl.* **1997**, 2235-2245.

[22] a) S. Salama, J. D. Stong, J. B. Neilands and T. G. Spiro, *Biochemistry* **1978**, *17*, 3781-3785; b) T. B. Karpishin, M. S. Gebhard, E. I. Solomon and K. N. Raymond, *J. Am. Chem. Soc.* **1991**, *113*, 2977-2984.

[23] a) Y. Cohen, L. Avram and L. Frish, *Angew. Chem. Int. Ed.* **2005**, *44*, 520-554; b) A. S. Altieri, D. P. Hinton and R. A. Byrd, *J. Am. Chem. Soc.* **1995**, *117*, 7566-7567.

[24] a) L. Avram and Y. Cohen, *Chem. Soc. Rev.* **2015**, *44*, 586-602; b) A. Macchioni, G. Ciancaleoni, C. Zuccaccia and D. Zuccaccia, *Chem. Soc. Rev.* **2008**, *37*, 479-489.

[25] a) N. Dalla Favera, L. Guenee, G. Bernardinelli and C. Piguet, *Dalton Trans.* **2009**, 7625-7638; b) B. M. Schulze, D. L. Watkins, J. Zhang, I. Ghiviriga and R. K. Castellano, *Org. Biomol. Chem.* **2014**, *12*, 7932-7936.

[26] a) F. Mohamadi, N. G. J. Richards, W. C. Guida, R. Liskamp, M. Lipton, C. Caufield, G. Chang, T. Hendrickson and W. C. Still, *J. Comput. Chem.* **1990**, *11*, 440-467; b) S. J. Weiner, P. A. Kollman, D. A. Case, U. C. Singh, C. Ghio, G. Alagona, S. Profeta, Jr. and P. Weiner, *J. Am. Chem. Soc.* **1984**, *106*, 765-784.

[27] a) M. Albrecht, S. Mirtschin, M. de Groot, I. Janser, J. Runsink, G. Raabe, M. Kogej, C. A. Schalley and R. Fröhlich, *J. Am. Chem. Soc.* **2005**, *127*, 10371-10387; b) A. Marquis-Rigault, A. Dupont-Gervais, P. N. W. Baxter, A. Van Dorsselaer and J.-M. Lehn, *Inorg. Chem.* **1996**, *35*, 2307-2310.

[28] I. Kolossváry and W. C. Guida, *J. Am. Chem. Soc.* **1996**, *118*, 5011-5019.

[29] a) A. Braibanti, G. Ostacoli, P. Paoletti, L. D. Pettit and S. Sammartano, *Pure Appl. Chem.* **1987**, *59*, 1721-1728; b) K. A. Connors, *Binding Constants: The Measurements of Molecular Complex Stability*, John Wiley & Sons, New York, **1987**, p; c) P. Gans, A. Sabatini and A. Vacca, *Talanta* **1996**, *43*, 1739-1753; d) P. Gans, A. Sabatini and A. Vacca, *Ann. Chim.* **1999**, *89*, 45-49.

[30] a) H. J. Hogben, J. K. Sprafke, M. Hoffmann, M. Pawlicki and H. L. Anderson, *J. Am. Chem. Soc.* **2011**, *133*, 20962-20969; b) C.-H. Lee, H. Yoon, P. Kim, S. Cho, D. Kim and W.-D. Jang, *Chem. Commun.* **2011**, *47*, 4246-4248; c) J. Wang, D.-T. Pham, T. W. Kee, S. N. Clafton, X. Guo, P. Clements, S. F. Lincoln, R. K. Prud'homme and C. J. Easton, *Macromolecules* **2011**, *44*, 9782-9791; d) S. Brahma, S. A. Ikbal, A. Dhamija and S. P. Rath, *Inorg. Chem.* **2014**, *53*, 2381-2395; e) D. Shimoyama, H. Yamada, T. Ikeda, R. Sekiya and T. Haino, *Eur. J. Org. Chem.* **2016**, 3300-3303; f) P. Mondal, S. Sarkar and S. P. Rath, *Chem. Eur. J.* **2017**, *23*, 7093-7103; g) L. K. S. von Krbek, A. J. Achazi, S. Schoder, M. Gaedke, T. Biberger, B. Paulus and C. A. Schalley, *Chem. Eur. J.* **2017**, *23*, 2877-2883; h) Y.-L. Ma, H. Ke, A. Valkonen, K. Rissanen and W. Jiang, *Angew. Chem. Int. Ed.* **2018**, *57*, 709-713.

[31] T. B. Karpishin, T. D. P. Stack and K. N. Raymond, *J. Am. Chem. Soc.* **1993**, *115*, 6115-6125.

[32] a) J. van Gestel, *Macromolecules* **2004**, *37*, 3894-3898; b) J. van Gestel, *J. Phys. Chem. B* **2006**, *110*, 4365-4370.

[33] a) M. M. Green, J.-W. Park, T. Sato, A. Teramoto, S. Lifson, R. L. B. Selinger and J. V. Selinger, *Angew. Chem. Int. Ed.* **1999**, *38*, 3138-3154; b) A. R. A. Palmans and E. W. Meijer, *Angew. Chem. Int. Ed.* **2007**, *46*, 8948-8968.

[34] a) M. M. Green, N. C. Peterson, T. Sato, A. Teramoto, R. Cook and S. Lifson, *Science* **1995**, *268*, 1860-1866; b) R. Nonokawa and E. Yashima, *J. Am. Chem. Soc.* **2003**, *125*, 1278-1283; c) B. Isare, M. Linares, L. Zargarian, S. Fermandjian, M. Miura, S. Motohashi, N. Vanthuyne, R. Lazzaroni and L. Bouteiller, *Chem. Eur. J.* **2010**, *16*, 173-177; d) M. M. J. Smulders, I. A. W. Filot, J. M. A. Leenders, P. van der Schoot, A. R. A. Palmans, A. P. H. J. Schenning and E. W. Meijer, *J. Am. Chem. Soc.* **2010**, *132*, 611-619; e) T. Kim, T. Mori, T. Aida and D. Miyajima, *Chem. Sci.* **2016**, *7*, 6689-6694; f) Y. Tsunoda, M. Takatsuka, R. Sekiya and T. Haino, *Angew. Chem. Int. Ed.* **2017**, *56*, 2613-2618.

10.1002/chem.201800997

WILEY-VCH

Entry for the Table of Contents (Please choose one layout)

FULL PAPER

Triple helices: Calix[4]arene-based triple-stranded metallohelicates encapsulate cationic guests within the binding cavities, which are conformationally coupled. Their cooperative guest binding directs the allosteric effect and majority-rules effect in the molecular recognition.

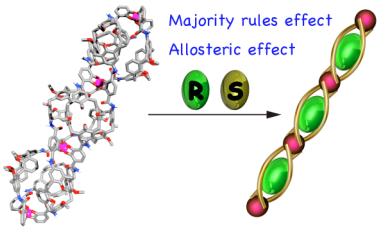

*Yutaro Yamasaki, Hidemi Shio, Tomoko Amimoto, Ryo Sekiya and Takeharu Haino**

Page No. – Page No.

Majority-Rules Effect and Allostery in Molecular Recognition of Calix[4]arene-Based Triple-Stranded Metallohelicates